Biodegradation (2012) 23:525–534
DOI 10.1007/s10532-011-9530-9

ORIGINAL PAPER

A biogeochemical framework for bioremediation of plutonium(V) in the subsurface environment

Randhir P. Deo · Bruce E. Rittmann

Received: 10 September 2011 / Accepted: 17 December 2011 / Published online: 1 January 2012

Abstract Accidental release of plutonium (Pu) from storage facilities in the subsurface environment is a concern for the safety of human beings and the environment. Given the complexity of the subsurface environment and multivalent state of Pu, we developed a quantitative biogeochemical framework for bioremediation of $Pu(V)O_2^+$ in the subsurface environment. We implemented the framework in the biogeochemical model CCBATCH by expanding its chemical equilibrium for aqueous complexation of Pu and its biological sub-models for including Pu's toxicity and reduction reactions. The quantified framework reveals that most of the Pu(V) is speciated as free $Pu(V)O_2^{+}{}_{(aq)}$, which is a problem if the concentration of free $Pu(V)O_2^+$ is $\geq$28 μM (the half-maximum toxicity value for bacteria able to reduce Pu(V) to $Pu(III)PO_{4(am)}$) or $\geq$250 μM (the full-toxicity value that takes the bioreduction rate to zero). The framework includes bioreduction of Fe^{3+} to Fe^{2+}, which abiotically reduces $Pu(V)O_2^+$ to Pu(IV) and then to Pu(III). Biotic (enzymatic) reduction of $Pu(V)O_2^+$ directly to Pu(III) by *Shewanella alga* (*S. alga*) is also included in the framework. Modeling results also reveal that for formation of $Pu(III)PO_{4(am)}$, the desired immobile product, the concentration of coexisting model strong ligand—nitrilotriacetic acid (NTA)—should be less than or equal to the concentration of total Pu(III).

Keywords Plutonium · *Shewanella alga* (*S. alga*) · Modeling · Biogeochemical framework · Bioreduction · Bioremediation

R. P. Deo (✉)
Chemistry Department, Division of Natural Sciences, College of Natural and Applied Sciences, University of Guam, Mangilao, GU 96923, USA
e-mail: rdeo@uguam.uog.edu

B. E. Rittmann
Center for Environmental Biotechnology, Biodesign Institute at Arizona State University, Tempe, AZ 85287-5701, USA

Introduction

Plutonium (Pu) from the nuclear-energy and weapons industries poses important risks. Although used (waste) Pu is stored in fuel rods underground, accidental release of Pu from these stored facilities [estimated at 1.6×10^{16} Bq (Choppin and Bond 1996)] is a major concern for humans and the environment, especially since Pu has a long half-life (2.4×10^4 years) and is capable of radiolytic and chemical toxicity (Demirkanli et al. 2007; Neu et al. 2005; Reed et al. 2010).

Once released in the subsurface environment, Pu may occur in any of five oxidation states, depending on the biogeochemistry of the subsurface environment. This results in complicated Pu chemistry, since the chemical speciation and mobility of Pu differ among the oxidation states (Demirkanli et al. 2007;

Reed et al. 2010). For example, under oxidizing conditions, plutonium occurs as $Pu(V)O_2^+$ and $Pu(VI)O_2^{2+}$, which form distinct complexes with inorganic/organic compounds (Choppin 2003; Cleveland and Rees 1981). While $Pu(VI)O_2^{2+}$ forms strong hydroxyl complexes and sorbs strongly to aquifer surfaces, $Pu(V)O_2^+$ does not form hydroxyl complexes until pH >8 and, therefore, should be very mobile under most subsurface conditions (Choppin 2003; Francis 2007; Reed et al. 2010).

The best strategy to avoid unintentional exposure from Pu is to convert it to a precipitate phase that is immobile in the subsurface environment. For actinides (An) in general, lower oxidation states—An(III) and An(IV)—are less soluble and are more likely to precipitate than are the higher oxidation states. For plutonium, Pu(IV) and Pu(III) oxidation states exhibit lower solubility and, thus, are the target oxidation states (Banaszak et al. 1999; Francis 2007; Reed et al. 2010).

If the chemical and redox speciation of Pu in the subsurface environment is dominated by soluble oxidized forms, reduction of Pu to the more desired Pu(III) or Pu(IV) oxidation states is a remediation option. Fortunately, microbial reduction of Pu has been reported under anaerobic conditions: by *Bacillus polymyxa* and *circulans* (Rusin et al. 1994), *Geobacter metallireducens* GS15 and *Shewanella oneidensis* MR1 (Boukhalfa et al. 2007; Icopini et al. 2009), *Clostridium* sp. (Francis et al. 2008), and *Shewanella alga* (*S. alga*) (Reed et al. 2007).

In this work, we develop a quantitative biogeochemical framework for assessing bioremediation of $Pu(V)O_2^+$ in the subsurface environment. First, we evaluate the chemical speciation of $Pu(V)O_2^+$, which is the most problematic form of oxidized Pu, since it is more soluble and thus mobile than Pu(VI). Second, we evaluate the toxicity of $Pu(V)O_2^+$ towards *S. alga*. Third, we introduce direct and indirect microbial reduction of $Pu(V)O_2^+$ to form Pu(IV) and Pu(III) products. Fourth, we evaluate the chemical speciation of the reduced products, placing special attention on the effect of nitrilotriacetic acid (NTA), a strong complexing ligand, towards production of immobile Pu(III) precipitate phase, the desired end product. NTA is a key inclusion in this study. On the one hand, strong complexing ligands, such as NTA, are known to coexist in plutonium contaminated sites (Banaszak et al. 1998a, b; Boukhalfa et al. 2007). On the other hand, this study shows that equimolar concentrations of NTA and Fe(III) is essential to keep Fe(III) in soluble form.

Modeling

Background information on the biogeochemical model CCBATCH

We develop the biogeochemical framework for bioremediation of Pu by building upon the biogeochemical model CCBATCH, which was developed by our team to quantitatively link all the different types of reactions that control the fate of radionuclides and a range of other metals and organic co-contaminants (Banaszak et al. 1998b; Rittmann and VanBriesen 1996; Rittmann et al. 2002a, b; Schwarz and Rittmann 2007a, b; VanBriesen and Rittmann 2000a, b; Willett and Rittmann 2003). The basic structure of CCBATCH is described here, and critical details, such as parameter values, are reported as needed in "Results and Discussion".

CCBATCH explicitly couples biological electron-donor and -acceptor consumptions to simultaneous chemical reactions, including acid/base, complexation, and precipitation. In this way, CCBATCH directly links the effects of biological reactions to the biogeochemical fate of various components in the system, even when the components do not participate directly in the biological reaction. The original CCBATCH model coupled kinetically controlled microbial reactions with thermodynamically controlled aqueous phase acid/base and complexation reactions (VanBriesen and Rittmann 1999, 2000a). Subsequently, Rittmann et al. (2002b) added a sub-model to link kinetically or equilibrium-controlled precipitation/dissolution to the microbial and aqueous-phase reactions. Willett and Rittmann (2003) also added a sub-model to link slow kinetically controlled complexation to bioavailability of organic ligands for microbial reactions. Schwarz and Rittmann (2007a, b) expanded the CCBATCH model to transport of contaminants. Recently, Marcus et al. (2010) expanded the CCBATCH platform to biofilms, including those that live on the anode of a microbial fuel cell.

All the equilibrium reactions in CCBATCH are solved by a Newton–Raphson technique that combines the aqueous-phase mass balances with mass-action equilibrium expressions for all relevant acid/base and complexation reactions, and it can compute the

equilibrium pH from the proton condition when the pH is not fixed. Thus, changes in acidic hydrogen during biological reactions and precipitation/dissolution reactions are explicitly captured by the proton condition (VanBriesen and Rittmann 1999).

Modeling domain and utilized feature of CCBATCH

We develop our biogeochemical framework for Pu bioremediation for a batch system using previously reported experimental (Reed et al. 2007) and modeling (Deo et al. 2011) results. Table 1 describes the components of the medium used for the batch reactions. Furthermore, we use the following features of CCBATCH for our framework:

- Chemical equilibrium sub-model—represents thermodynamically controlled, aqueous phase acid/base and complexation reactions among medium components.
- Biological sub-model—represents kinetically controlled microbial oxidation/reduction reactions with $Pu(V)O_2^+$ and other biologically active components of the medium, and provides stoichiometric links to the production and consumption of other components.
- Precipitation/dissolution sub-model—uses the thermodynamically controlled (equilibrium) feature for representing precipitation/dissolution of Pu component that can form solids.

Table 1 Identity and concentrations of initial components of the medium used in this study (Adapted from Reed et al. (2007))

Aqueous species	Concentration (mM)
K^+	12.4
NH_4^+	11.22
Cl^-	43.1
Lactate	20
PuO_2^+	0.01
Total carbonate	2.0
NTA^{3-}	10
Fe^{3+}	10
S. alga	0.00418
Mg^{2+}, Mn^{2+}, SO_4^{2+}, Ca^{2+}, Co^{2+}, Zn^{2+}, Cu^{2+}, Al^{3+}, borate, MoO_4^{2-}, Ni^{2+}, WO_4^{2-}, PO_4^{3-}, NO_3^-	Trace levels

The following are the components we modeled: lactate, acetate, H^+, Fe^{3+}, Fe^{2+}, *Shewanella alga* (*S. alga*), $Pu(V)O_2^+$, $Pu(IV)^{4+}$, and $Pu(III)^{3+}$. We chose *S. alga* as our model bacterium for driving the biological reactions, since it has well characterized kinetics for the components and reactions we consider (Caccavo et al. 1992, 1996; Liu et al. 2002; Songkasiri 2003; Truex et al. 1997).

Upgrading CCBATCH for chemical speciation of $Pu(V)O_2^+$

To use CCBATCH for this domain, we needed to expand the model to include the chemical (equilibrium) reactions of Pu (i.e., $Pu(V)O_2^+$, $Pu(IV)^{4+}$, and $Pu(III)^{3+}$) with other components in the medium (Table 1). We added complexes of $Pu(V)O_2^+$, $Pu(IV)^{4+}$, and $Pu(III)^{3+}$ with the common components of the medium, along with their respective equilibrium constants and stoichiometric mass balances; the complexes and formation constants are listed in Table 2.

Reduction of $Pu(V)O_2^+$ by Shewanella alga

We chose Pu(III) as the final reduced form of plutonium based on literature reports that support $Pu(V)O_2^+$ reduction to Pu(III) under anaerobic conditions by metal-reducing bacteria: *Geobacter metallireducens* GS15 and *Shewanella oneidensis* MR1 (Boukhalfa et al. 2007), *Geobacter sulfurreducens* and *Shewanella oneidensis* (Renshaw et al. 2009), and *Clostridium* sp. (Francis et al. 2008).

When modeling $Pu(V)O_2^+$ reduction in the presence of Fe(III)-NTA in the medium, we hypothesized that $Pu(V)O_2^+$ reduction is abiotic (chemical), being directly due to Fe(II) that is produced upon preferential biological reduction of Fe(III) (Reed et al. 2007). Also, we included that $Pu(V)O_2^+$ follows a stepwise reduction to Pu(IV) and then to Pu(III). Based on these hypotheses, we linked microbial reduction of Fe(III) to Fe(II), to abiotic reduction of $Pu(V)O_2^+$ to Pu(IV), and then to Pu(III).

Table 3 summarizes the parameters that describe the bioreduction of Fe(III) and *S. alga* growth from it: $q_{lactate}$ = maximum specific rate of lactate utilization, $K_{a,Fe(III)}$ = electron acceptor concentration that gives half of the maximum growth rate, and b = first-order endogenous-decay rate. The yield and stoichiometry for all components involved in Fe(III) bioreduction

Table 2 Formation constants for major Pu(V, IV, III) aqueous complexes at ionic strength = 0.1

Species	Log K	Ref.
$Pu(V)O_2CO_3^-$	5.12	Smith et al. (2004)
$Pu(V)O_2(CO_3)_2^{3-}$	6.5	Gustafsson (2009)
$Pu(V)O_2(CO_3)_3^{5-}$	5.5	Gustafsson (2009)
$Pu(V)O_2OH$	−9.7	Gustafsson (2009)
$Pu(V)O_2NTA$	6.75	Banaszak et al. (1999)
$Pu(IV)(CO_3)_4^{4-}$	34.1	Gustafsson (2009)
$Pu(IV)(CO_3)_5^{6-}$	32.7	Gustafsson (2009)
$Pu(IV)(OH)_2^{2+}$	0.6	Gustafsson (2009)
$Pu(IV)(OH)_3^+$	−2.3	Gustafsson (2009)
$Pu(IV)(OH)_4$	−8.6	Gustafsson (2009)
$Pu(IV)NTA^+$	12.82	Banaszak et al. (1999)
$Pu(IV)(SO_4)^{2+}$	5.5	Gustafsson (2009)
$Pu(III)\ (OH)_2^+$	−7	Gustafsson (2009)
$Pu(III)\ (CO_3)^+$	8.1	Gustafsson (2009)
$Pu(III)\ (CO_3)_2^-$	12.9	Gustafsson (2009)
$Pu(III)\ (CO_3)_3^{3-}$	15.4	Gustafsson (2009)
Pu(III)NTA	12.2	Gustafsson (2009)
$Pu(III)PO_{4(am)}$	Log $K_{sp} = -24.6$	Gustafsson (2009)

were based on the following overall reaction for lactate utilization coupled to biomass synthesis (Rittmann and McCarty 2001):

$$0.25\ CH_3CHOHCOO^- + 0.77\ Fe^{3+} + 0.0115\ NH_4^+ \rightarrow 0.0115\ C_5H_7O_2N + 0.25\ CH_3COO^- + 0.1925\ H_2CO_3 + 0.7815\ H^+ + 0.77\ Fe^{2+} \quad (1)$$

We assumed that the lactate concentration is in excess, which means that the kinetics is controlled by the concentration of available Fe(III). We also assumed that the available Fe(III) equals the total Fe(III), since the medium's pH was buffered at pH 7, which fixed the relative concentration of any Fe(III) species with total Fe(III). Equation 1 is represented in the model by the rate of substrate (i.e., lactate) utilization using the following rate expression:

$$\text{Rate}_{(\text{lactate})} = q_{\text{lactate}} \times [\text{S. alga}] \times \left(\frac{[\text{Fe(III)}]}{[\text{Fe(III)}] + K_{a,\text{Fe(III)}}}\right) \quad (2)$$

in which q_{lactate} = maximum specific rate of lactate utilization, $K_{a,\text{Fe(III)}}$ = electron acceptor concentration that gives half of the maximum growth rate, and [*S. alga*] and [Fe(III)] represent concentrations of *S. alga* and Fe(III), respectively. Then, rates of consumption or production of other species in eq. 1 were calculated using their stoichiometry normalized to lactate. For example, rate of biomass (i.e., *S. alga*) synthesis is:

$$\text{Rate}_{(\text{S. alga})} = \text{Rate}_{\text{lactate}} \times \left(\frac{0.0115}{0.25}\right) \quad (3)$$

Since *S. alga* is also lost to cell death and endogenous respiration, collectively called cell decay, we represented the net rate of *S. alga* formation with the following expression:

$$\text{Net Rate}_{(\text{S. alga})} = \text{Rate}_{\text{lactate}} \times \left(\frac{0.0115}{0.25}\right) - (b \times [\text{S. alga}]) \quad (4)$$

Following microbial reduction of Fe(III), the produced Fe(II) was linked to abiotic reductions of $Pu(V)O_2^+$ to Pu(IV) and then Pu(IV) to Pu(III). We represented these abiotic reductions using the following overall reactions:

$$Pu(V)O_2^+ + Fe^{2+} + 4H^+ \rightarrow Fe^{3+} + Pu(IV)^{4+} + 2H_2O \quad (5)$$

$$Pu(IV)^{4+} + Fe^{2+} \rightarrow Fe^{3+} + Pu(III)^{3+} \quad (6)$$

For these reactions, we assumed first-order kinetics with respect to $Pu(V)O_2^+$, $Pu(IV)^{4+}$, and Fe^{2+} concentrations:

$$\text{Rate} = k_1 \left[Pu(V)O_2^+\right] \left[Fe^{2+}\right] \quad (7)$$

$$\text{Rate} = k_2 \left[Pu(IV)^{4+}\right] \left[Fe^{2+}\right] \quad (8)$$

In the absence of Fe(III)-NTA to keep Fe is solution, we included in the model reduction of

Table 3 Kinetic parameters for biotic reduction of Fe^{3+}, and abiotic reductions of $Pu(V)O_2^+$ and Pu^{4+}

Parameter	Value	How estimated
q_{lactate}	77.9 mol Lac. (mol cell × h)$^{-1}$	Deo et al. (2011)
$K_{a,\text{Fe(III)}}$	4.3×10^{-3} M	Deo et al. (2011)
b	0.024 day^{-1}	Hacherl and Kosson (2003)
k_1	26.25 M^2 h^{-1}	Deo et al. (2011)
k_2	26.25 M^2 h^{-1}	Deo et al. (2011)
k_3	0.892 M h^{-1}	Deo et al. (2011)
$KPuO_2^+$	2.8×10^{-5} M	Banaszak et al. (1998b)

$Pu(V)O_2^+$ to Pu(III) by direct (enzymatic) reduction reaction (Deo et al. 2011; Reed et al. 2007). The yield and stoichiometry for all components involved in $Pu(V)O_2^+$ bioreduction were based on the following overall reaction that couples Pu(V) reduction to lactate utilization:

$$0.25\ CH_3CHOHCOO^- + 0.5\ Pu(V)O_2^+ + H^+ \rightarrow 0.25\ CH_3COO^- + 0.25\ H_2CO_3 + 0.5\ Pu(III)^{3+} + 0.5\ H_2O \quad (9)$$

The kinetic parameters that describe $Pu(V)O_2^+$ reductions—k_1 = abiotic reduction of $Pu(V)O_2^+$ to $Pu(IV)^{4+}$, k_2 = abiotic reduction rate of $Pu(IV)^{4+}$ to $Pu(III)^{3+}$, and k_3 = rate constant of biotic reduction of $Pu(V)O_2^+$ to $Pu(III)^{3+}$ without supporting growth of *S. alga*—are given in Table 3. We assumed first-order kinetics with respect to the $Pu(V)O_2^+$ concentration for biotic reduction of $Pu(V)O_2^+$ to $Pu(III)^{3+}$:

$$\text{Rate} = k_3\left[Pu(V)O_2^+\right] \quad (10)$$

Toxicity of $Pu(V)O_2^+$ towards Shewanella alga

Since actinides have shown toxicity towards bacteria at elevated concentrations (Reed et al. 2010), we included toxicity of $Pu(V)O_2^+$ in the model. For example, Banaszak et al. (1998b) reported that free $NpO_2^+{}_{(aq)}$ above 2.8×10^{-5} M was toxic towards *Chelatobacter heinstzii*, while Reed et al. (2007) reported loss of *S. alga* cell viability with increasing concentrations of Pu(V) in PIPES buffer at pH 7. The loss of *S. alga* cell viability, however, was minimized in the presence of strong chelating agents, including NTA. From this observation, we infer that the toxicity was due to availability of free $Pu(V)O_2^+{}_{(aq)}$, which concentration was reduced upon complexation with the added NTA. In this study, we added the following toxicity effect to rate eqs. 2 and 10, respectively, in the presence or absence of Fe^{3+}-NTA:

$$\frac{KPu(V)O_2^+}{KPu(V)O_2^+ + \left[Pu(V)O_2^+\right]} \quad (11)$$

where $KPu(V)O_2^+$ is the half-maximum toxicity concentration, and $[Pu(V)O_2^+]$ is the concentration of the free $Pu(V)O_2^+{}_{(aq)}$. We assumed the value of $KPu(V)O_2^+$ to be 2.8×10^{-5} M (Table 3). This means that the lactate utilization rate is reduced by 50% when the concentration of free $Pu(V)O_2^+{}_{(aq)}$ is 2.8×10^{-5} M. Furthermore, the model causes the lactate utilization rate to be zero when the $Pu(V)O_2^+$ concentration is $\geq 2.5 \times 10^{-4}$ M, which represents the full toxicity value.

Results and discussion

Chemical speciation of $Pu(V)O_2^+$ with Fe^{3+}-NTA

Figure 1 compares speciation of 10 μM $Pu(V)O_2^+$ when the medium is buffered at pH 7. The major aqueous species of $Pu(V)O_2^+$, and the percentages of the Pu(V) species are 90.13% for $Pu(V)O_2^+$, 8.97% for $Pu(V)O_2CO_3^-$, 0.71% for $Pu(V)O_2NTA$, 0.18% for $Pu(V)O_2OH$, and <0.00% for $Pu(V)O_2(CO_3)_2^{3-}$ (1.49×10^{-10} M) and $Pu(V)O_2(CO_3)_3^{5-}$ (9.41×10^{-16} M). The high percentage of free $Pu(V)O_2^+{}_{(aq)}$ illustrates the lack of strength of the organic complexing compounds in the medium. Since free $Pu(V)O_2^+{}_{(aq)}$ is the toxic species, its dominance means that toxicity can be important if Pu(V) is not reduced rapidly by *S. alga*.

Toxicity of $Pu(V)O_2^+$ towards Shewanella alga

Figure 2 shows the availability of free $Pu(V)O_2^+{}_{(aq)}$ (*y*-axis) at different total $Pu(V)O_2^+$ (*x*-axis) concentrations of 10, 30, 50, 250, and 300 μM. Also shown on the figure are free $Pu(V)O_2^+{}_{(aq)}$ values representing half-maximum toxicity (i.e., $KPu(V)O_2^+$) and full toxicity (dashed lines). The results illustrate that the

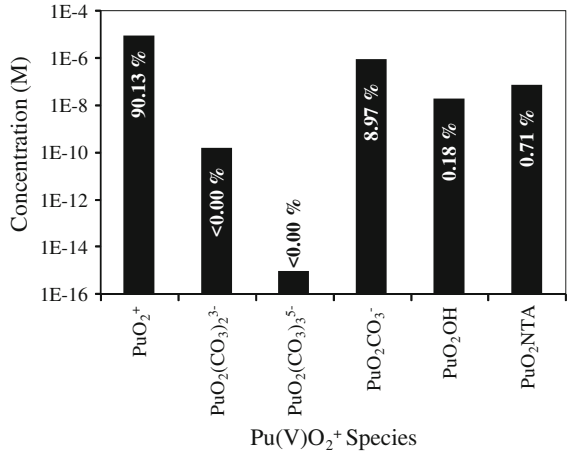

Fig. 1 Speciation of $Pu(V)O_2^+$ in the medium buffered at pH 7. Medium components are given in Table 1

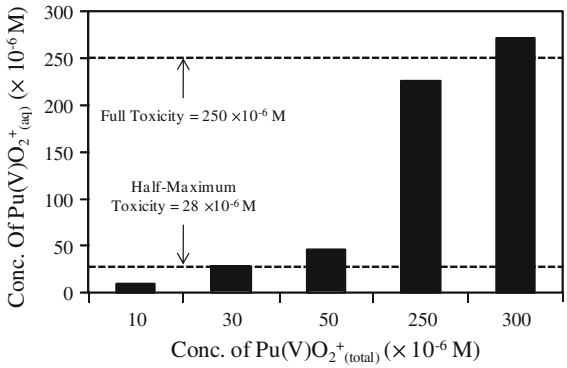

Fig. 2 Concentration of free (aquo) $Pu(V)O_2^+$ at different concentrations of total $Pu(V)O_2^+$ when present with 10 mM of Fe^{3+}-NTA. Also shown are values for half-maximum toxicity and full toxicity

free $Pu(V)O_2^+{}_{(aq)}$ concentration is more than the half-maximum toxicity value when the total $Pu(V)O_2^+$ concentration exceeds ~30 μM. When the total $Pu(V)O_2^+$ concentration reaches 300 μM, the available free $Pu(V)O_2^+{}_{(aq)}$ concentration is ~275 μM, which exceeds the full toxicity value.

The impact of toxicity is illustrated in Fig. 3, which shows the time course of the effect of $Pu(V)O_2^+$ toxicity on (Fig. 3A) production of Fe(II) (from biotic reduction of Fe(III)) at different total $Pu(V)O_2^+$ concentrations (μM) of 0, 10, 50, and 300. $Pu(V)O_2^+$ toxicity is reflected by the amount of Fe(II) produced, which is essential for abiotic reductions of $Pu(V)O_2^+$ to Pu(IV), and Pu(IV) to Pu(III). Also shown are the resultant abiotic reductions of $Pu(V)O_2^+$ in the absence (solid line) and presence (dashed line) of the toxicity effect at different initial $Pu(V)O_2^+$ concentrations of (Fig. 3) (B) 10 μM, (C) 50 μM, and (D) 300 μM. For a total $Pu(V)O_2^+$ concentration of 10 μM (Fig. 3B), Pu(V) reduction is only slightly affected by the presence of the toxicity term, since the free $Pu(V)O_2^+$ concentration is less than the half-maximum toxicity value. In Fig. 3C, Pu(V) reduction is delayed in the presence of the toxicity term, because the initial free $Pu(V)O_2^+$ concentration, ~49.6 μM out of a total $Pu(V)O_2^+$ concentration of 50 μM, is about twice the half-maximum toxicity value. At 300 μM (Fig. 3D), however, no $Pu(V)O_2^+$ is reduced, since the free $Pu(V)O_2^+$ concentration is more than the full-toxicity value of 250 μM, and the lactate utilization rate in the model is zero. These results show why including Pu(V) toxicity in the biogeochemical framework is essential for defining the upper limit of

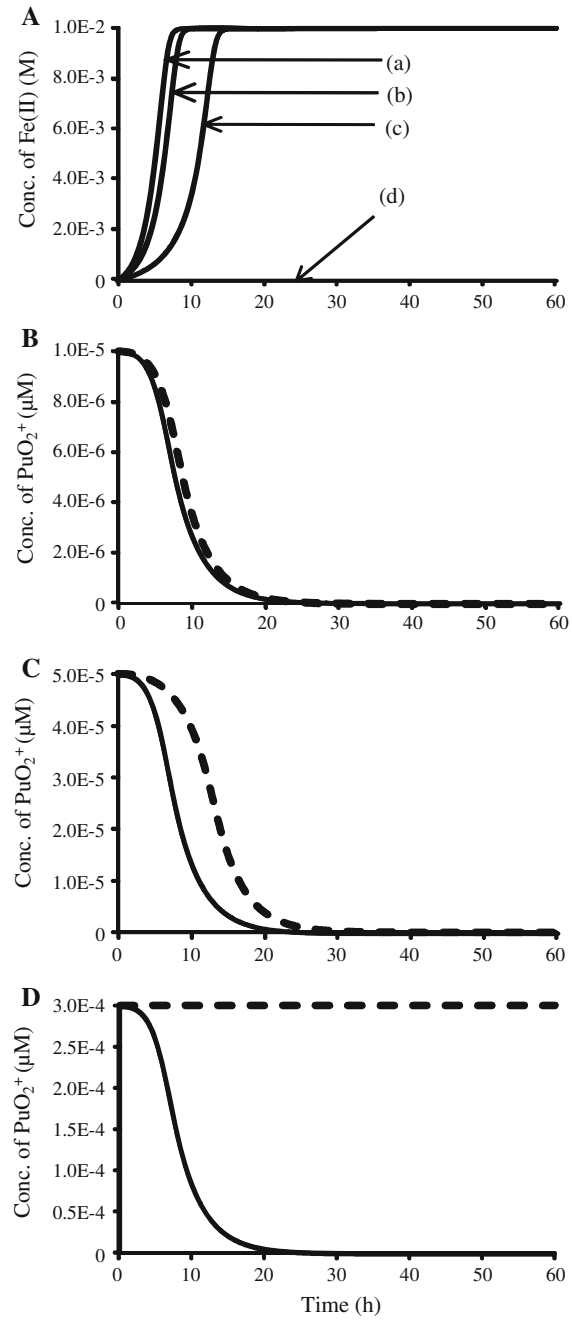

Fig. 3 **A** Effects of initial concentrations of total $Pu(V)O_2^+$ (μM)—(*a*) 0, (*b*) 10, (*c*) 50, (*d*) 300—on the production of Fe(II) (from reduction of Fe(III)). The resulting time course for the abiotic reduction of $Pu(V)O_2^+$ by the produced Fe(II) is also shown for different initial $Pu(V)O_2^+$ concentrations of **B** 10 μM, **C** 50 μM, **D** 300 μM, in the absence (*solid line*) and presence (*dashed line*) of the toxicity term (eq. 10)

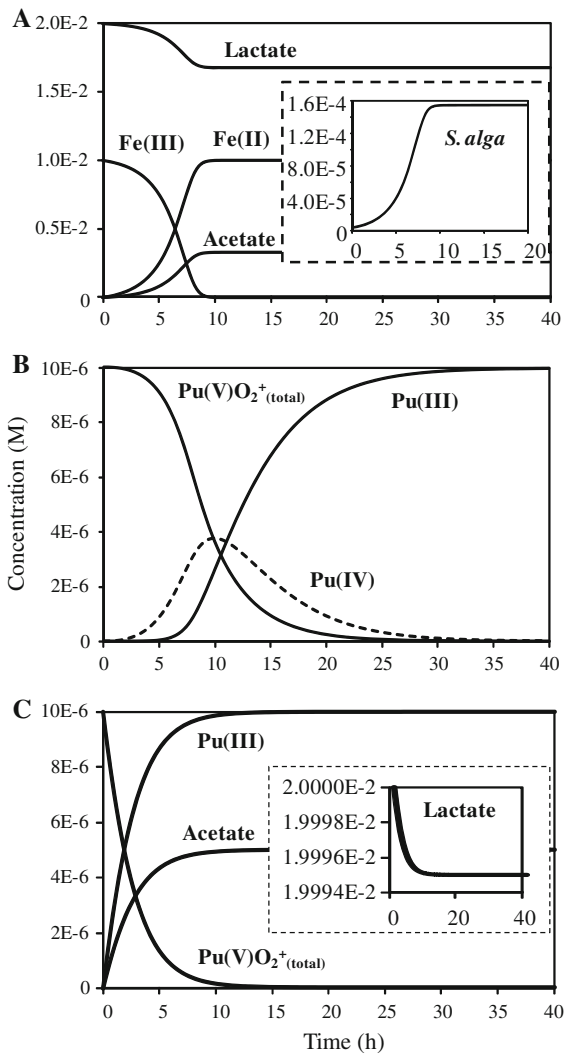

Fig. 4 **A** Model simulation for bioreduction of Fe(III) by *S. alga*. Also shown are consumption of lactate and productions of acetate and Fe(II), and growth of *S. alga* (inset). **B** Model simulation for concurrent abiotic reductions of $Pu(V)O_2^+$ to Pu(IV) and Pu(IV) to Pu(III) by the Fe(II) produced in **A**. **C** Model simulation for bioreduction of $Pu(V)O_2^+$ to Pu(III) by *S. alga* in the absence of Fe^{3+}-NTA. Also shown is production of acetate from oxidation of lactate, which is shown as inset

actinide concentration when designing effective bioremediation strategies.

Reduction of $Pu(V)O_2^+$ by Shewanella alga

With the toxicity effect established, we explore transformations of all the major components involved in reduction of $Pu(V)O_2^+$ to Pu(III). First is reduction of $Pu(V)O_2^+$ in the presence of Fe^{3+}-NTA, where Fe(III) undergoes preferential bioreduction to Fe(II). Figure 4A shows model simulations for transformations of all the major components during bioreduction of Fe(III). The results show complete reduction of Fe(III) to Fe(II) in ~10 h, along with stoichiometric consumption of lactate, productions of Fe(II) and acetate, and growth of *S. alga*. All the components reach plateaus after ~10 h due to complete consumption of all the available Fe(III), the limiting reactant.

Figure 4B shows model simulations for abiotic reduction of $Pu(V)O_2^+$ to Pu(IV) and Pu(III) that occurred in parallel with the results in Fig. 4A. Once significant Fe(II) has built up (at about 3 h), abiotic reduction of $Pu(V)O_2^+$ to Pu(IV) takes place. The reduction of Pu(IV) to Pu(III) is delayed to about 6 h, when enough Pu(IV) has accumulated so that its reduction of $Pu(V)O_2^+$ is observable. Most generation and consumption of Pu(IV) takes place between 5th and 25th h, and production of Pu(III) is complete by the 35th h. The maximum accumulation of Pu(IV) is ~37.5% of the total initial $Pu(V)O_2^+$, which reflects that abiotic reduction of $Pu(V)O_2^+$ and Pu(IV) occur simultaneously. An especially telling effect of having Pu reduction be abiotic is that reduction to Pu(III) requires ~35 h, even though the complete biotic reduction of Fe(III) is achieved in less than 10 h.

We also show reduction of $Pu(V)O_2^+$ in the absence of Fe^{3+}-NTA, where we assumed that $Pu(V)O_2^+$ is only enzymatically reduced directly to Pu(III) by *S. alga*. Figure 4C shows model simulations for bioreduction of $Pu(V)O_2^+$ to Pu(III) by *S. alga*, along with stoichiometric consumption of lactate and production of acetate. Modeling results indicate that full bioreduction of 10 μM of $Pu(V)O_2^+$ to Pu(III) is achieved in ~10 h, but with very little consumption of lactate (~0.025%), since Fe(III) could not be reduced.

While reduction of Pu was reported before (Rai et al. 2002; Reed et al. 2006), this framework model is the first to demonstrate mechanistic understanding of $Pu(V)O_2^+$ bioreduction in the absence and presence of Fe^{3+}-NTA. An especially unique feature is the stepwise reductions of $Pu(V)O_2^+$ to Pu(IV) and to Pu(III), along with its coupling to the biotic reactions that produce the Fe(II). The coupled biotic and abiotic mechanisms are important to understand when designing a bioremediation strategy for $Pu(V)O_2^+$ (Reed et al. 2007, 2010; Tabak et al. 2005). While the ultimate goal is to drive microbial reduction of

$Pu(V)O_2^+$ to the less soluble Pu(III) form, this goal may be achieved only in the absence of strong Pu(III)-complexing ligands, which would prevent Pu(III) from precipitating to form an immobile phase.

Thus, along with reduction of $Pu(V)O_2^+$ to Pu(III), we evaluated the fate of Pu(III) in a medium in which $Pu(V)O_2^+$ is reduced in the presence of Fe^{3+}-NTA. We used $Pu(III)PO_{4(am)}$ as an example for the precipitate phase of reduced Pu. Figure 5A shows model simulation for speciation of Pu(III) when the formation of a Pu(III) precipitate, $Pu(III)PO_{4(am)}$, is possible. Speciation results show that almost all the Pu(III) is speciated to $Pu(III)NTA_{(aq)}$ (99.94%), leaving minor amounts of $Pu(III)(CO_3)^+_{(aq)}$—0.01%—and $Pu(III)PO_{4(am)}$—0.05%. Since the dominant reduced form is highly soluble and, therefore, undesirable, the strategy of bioreduction of Pu(III) did not succeed when the medium contained NTA at a 1000:1 mol ratio with Pu; this high NTA:Pu ratio occurs when NTA is present to complex the much more abundant Fe(III). Similar undesired reduced products were observed experimentally, in the presence of comparable concentrations of chelating agents, upon reductions of uranium—forming a U(IV)-citric acid complex (Francis and Dodge 2008)—and plutonium—forming Pu(III)-EDTA (Boukhalfa et al. 2007) and Pu(III)-NTA (Rusin et al. 1994) complexes.

We explored the effects of reducing the concentration of NTA on the formation of $Pu(III)PO_{4(am)}$, the desired reduced product. The results in Fig. 5B indicate that decreasing the concentration of NTA from 10 to 0.01 mM allows the fraction of $Pu(III)PO_{4(am)}$ to increase from 98.5%, since almost all of the Pu(III) is free to complex with PO_4^{3-} to form $Pu(III)PO_{4(am)}$. Thus, $Pu(III)PO_{4(am)}$ becomes a promising immobilized form if NTA is minimized, for example, through biodegradation by *Chelatobacter heintzii* (Banaszak et al. 1998b). Our modeling results indicate that concentrations of strong complexing ligands, such as NTA, should be monitored, because having their concentration at more than a 1:1 molar ratio with Pu(III) can counteract the benefits of bioreduction of Pu.

Conclusions

We developed a biogeochemical framework for bioremediation of $Pu(V)O_2^+$ in the subsurface environment.

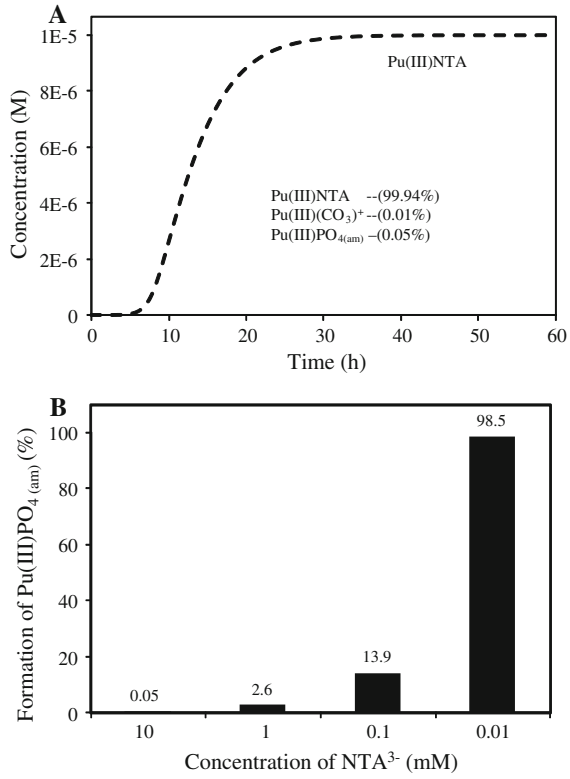

Fig. 5 **A** Speciation of Pu(III) in the presence of Pu(III) precipitate formation as $Pu(III)PO_{4(am)}$ in the medium of Table 1. **B** Percent formation of $Pu(III)PO_{4(am)}$ as a function of different concentrations of NTA

Initial chemical speciation revealed that most of Pu(V) was distributed as free $Pu(V)O_2^+{}_{(aq)}$ (99.40%). Since free $Pu(V)O_2^+$ is toxic towards bacteria, such high dominance of free $Pu(V)O_2^+$ limits the maximum free concentration of $Pu(V)O_2^+$ that can be bioremediated to ~250 μM. We then evaluated the reduction of $Pu(V)O_2^+$ by *S. alga* in the presence of Fe^{3+}-NTA. We assumed that *S. alga* reduces Fe(III) to Fe(II), which then abiotically reduces $Pu(V)O_2^+$ stepwise reduction to Pu(IV) and then to Pu(III). We also evaluated biotic (enzymatic) reduction of $Pu(V)O_2^+$ by *S. alga*, where we assumed that $Pu(V)O_2^+$ is reduced directly to Pu(III) without formation of Pu(IV). Chemical speciation of the reduced (Pu(III)) product results in formation of an undesired soluble Pu(III) species—$Pu(III)NTA_{(aq)}$. However, systematic reduction of the NTA concentration from 10 to 0.01 mM allowed an increase in the formation of the desired product, $Pu(III)PO_{4(am)}$, from 0.05 to 98.5%. The comprehensive biogeochemical framework model identifies mechanisms and chemical

species that are essential to know when designing a strategy to bioremediate Pu(V) toward the formation of an immobilized Pu(III) precipitate phase.

Acknowledgments The research was supported, in part, by Environmental Remediation Sciences Program (ERSP) of the United States Department of Energy.

References

Banaszak JE, Reed DT, Rittmann BE (1998a) Speciation-dependent toxicity of neptunium(V) toward *Chelatobacter heintzii*. Environ Sci Technol 32(8):1085–1091

Banaszak JE, VanBriesen JM, Rittmann BE, Reed DT (1998b) Mathematical modelling of the effects of aerobic and anaerobic chelate biodegradation on actinide speciation. Radiochim Acta 82:445–451

Banaszak JE, Rittmann BE, Reed DT (1999) Subsurface interactions of actinide species and microorganisms: implications for the bioremediation of actinide-organic mixtures. J Radioanal Nucl Chem 241(2):385–435

Boukhalfa H, Icopini GA, Reilly SD, Neu MP (2007) Plutonium(IV) reduction by the metal-reducing bacteria *Geobacter metallireducens* GS15 and *Shewanella oneidensis* MR1. Appl Environ Microbiol 73(18):5897–5903

Caccavo F, Blakemore RP, Lovley DR (1992) A hydrogen-oxidizing, Fe(III)-reducing microorganism from the Great Bay estuary, New Hamshire. Appl Environ Microbiol 58(10):3211–3216

Caccavo F, Ramsing NB, Costerton JW (1996) Morphological and metabolic responses to starvation by the dissimilatory metal-reducing bacterium *Shewanella alga* BrY. Appl Environ Microbiol 62(12):4678–4682

Choppin GR (2003) Actinide speciation in the environment. Radiochim Acta 91:645–649

Choppin GR, Bond AH (1996) Actinide oxidation state speciation. J Anal Chem 51(12):1129–1138

Cleveland JM, Rees TF (1981) Characterization of plutonium in Maxey Flats radioactive trench leachates. Science 212(4502): 1506–1509

Demirkanli DI, Molz FJ, Kaplan DI, Fjeld RA, Serkiz SM (2007) Modeling long-term plutonium transport in the Savannah River Site vadose zone. Vadose Zone J 6(2): 344–353

Deo RP, Rittmann BE, Reed DT (2011) Bacterial Pu(V) reduction in the absence and presence of Fe(III)-NTA: modeling and experimental approach. Biodegradation 22:921–929

Francis AJ (2007) Microbial mobilization and immobilization of plutonium. J Alloys Compd 444:500–505

Francis AJ, Dodge CJ (2008) Bioreduction of uranium(VI) complexed with citric acid by *Clostridia* affects its structure and solubility. Environ Sci Technol 42(22):8277–8282

Francis AJ, Dodge CJ, Gillow JB (2008) Reductive dissolution of Pu(IV) by *Clostridium* sp. under anaerobic conditions. Environ Sci Technol 42(7):2355–2360

Gustafsson JP (2009) Visual MINTEQ: version 2.61. KTH, Department of Land and Water Resources Engineering, Stockholm

Hacherl EL, Kosson DS (2003) A kinetic model for bacterial Fe(III) oxide reduction in batch cultures. Water Resour Res 39: HWC 3-1

Icopini GA, Lack JG, Hersman LE, Neu MP, Boukhalfa H (2009) Plutonium(V/VI) reduction by the metal-reducing bacteria *Geobacter metallireducens* GS-15 and *Shewanella oneidensis* MR-1. Appl Environ Microbiol 75(11):3641–3647

Liu CX, Gorby YA, Zachara JM, Fredrickson JK, Brown CF (2002) Reduction kinetics of Fe(III), Co(III), U(VI), Cr(VI) and Tc(VII) in cultures of dissimilatory metal-reducing bacteria. Biotechnol Bioeng 80(6):637–649

Marcus AK, Torres CI, Rittmann BE (2010) Evaluating the impacts of migration in the biofilm anode using the model PCBIOFILM. Electrochim Acta 55(23):6964–6972

Neu MP, Icopini GA, Boukhalfa H (2005) Plutonium speciation affected by environmental bacteria. Radiochim Acta 93(11):705–714

Rai D, Gorby YA, Fredrickson JK, Moore DA, Yui M (2002) Reductive dissolution of PuO_2(am): the effect of Fe(II) and hydroquinone. J Solut Chem 31(6):433–453

Reed DT, Lucchini JF, Aase SB, Kropf AJ (2006) Reduction of plutonium(VI) in brine under subsurface conditions. Radiochim Acta 94(9–11):591–597

Reed DT, Pepper SE, Richmann MK, Smith G, Deo R, Rittmann BE (2007) Subsurface bio-mediated reduction of higher-valent uranium and plutonium. J Alloy Compd 444: 376–382

Reed DT, Deo RP, Rittmann BE (2010) Subsurface interactions of actinide species with microorganisms. In: Morss LR, Edelstein NM, Fuger J (eds) The chemistry of the actinide and transactinide elements, vol 6. Springer, New York (In press)

Renshaw JC, Law N, Geissler A, Livens FR, Lloyd JR (2009) Impact of the Fe(III)-reducing bacteria *Geobacter sulfurreducens* and *Shewanella oneidensis* on the speciation of plutonium. Biogeochemistry 94(2):191–196

Rittmann BE, McCarty PL (2001) Environmental biotechnology: principles and applications. The McGraw-Hill Companies Inc, New York 10020

Rittmann BE, VanBriesen JM (1996) Microbiological processes in reactive modeling. React Transp Porous Media 34: 311–334

Rittmann BE, Banaszak JE, VanBriesen JM, Reed DT (2002a) Mathematical modeling of precipitation and dissolution reactions in microbiological systems. Biodegradation 13(4):239–250

Rittmann BE, Banaszak JE, Reed DT (2002b) Reduction of Np(V) and precipitation of Np(IV) by an anaerobic microbial consortium. Biodegradation 13(5):329–342

Rusin PA, Quintana L, Brainard JR, Strietelmeier BA, Tait CD, Ekberg SA, Palmer PD, Newton TW, Clark DL (1994) Solubilization of plutonium hydrous oxide by iron-reducing bacteria. Environ Sci Technol 28(9):1686–1690

Schwarz AO, Rittmann BE (2007a) A biogeochemical framework for metal detoxification in sulfidic systems. Biodegradation 18(6):675–692

Schwarz AO, Rittmann BE (2007b) Modeling bio-protection and the gradient-resistance mechanism. Biodegradation 18(6):693–701

Smith RM, Martell AE, Motekaitis RJ (2004) NIST critically selected stability constants of metal complexes database,

Version 4.0, NIST: Standard Reference Data Program, Gaithersburg

Songkasiri W (2003) Biological processes in nuclear waste treatment: bio-reduction and bio-sorption of actinides. Northwestern University, Evanston

Tabak HH, Lens P, van Hullebusch ED, Dejonghe W (2005) Developments in bioremediation of soils and sediments polluted with metals and radionuclides – 1. Microbial processes and mechanisms affecting bioremediation of metal contamination and influencing metal toxicity and transport. Rev Environ Sci Biotechnol 4:115–156

Truex MJ, Peyton BM, Valentine NB, Gorby YA (1997) Kinetics of U(VI) reduction by a dissimilatory Fe(III)-reducing bacterium under non-growth conditions. Biotechnol Bioeng 55(3):490–496

VanBriesen JM, Rittmann BE (1999) Modeling speciation effects on biodegradation in mixed metal/chelate systems. Biodegradation 10(5):315–330

VanBriesen JM, Rittmann BE (2000a) Mathematical description of microbiological reactions involving intermediates. Biotechnol Bioeng 67(1):35–52

VanBriesen JM, Rittmann BE (2000b) Modeling biogeochemical interactions in co-contaminant systems. Abstracts of Papers of the American Chemical Society 220, U338

Willett AI, Rittmann BE (2003) Slow complexation kinetics for ferric iron and EDTA complexes make EDTA non-biodegradable. Biodegradation 14(2):105–121